Li *et al. J Wood Sci* (2020) 66:8
https://doi.org/10.1186/s10086-020-1851-z

Journal of Wood Science

ORIGINAL ARTICLE

Open Access

# Structural, chemical, and multi-scale mechanical characterization of waste windmill palm fiber (*Trachycarpus fortunei*)

Jing Li[1,2,3], Xuexia Zhang[4], Jiawei Zhu[2,3], Yan Yu[4] and Hankun Wang[2,3*]

**Abstract**

This study investigated the structural, chemical, and multi-scale mechanical properties of windmill palm (*Trachycarpus fortunei*) leaf sheath fiber, which were frequently wasted. Significant variation was observed in fiber diameter and cross-sectional morphology among different layers in a single leaf sheath, whereas the chemical composition, relative crystallinity index, and the microfibrillar angle (MFA) of palm fibers were almost the same among different layers. Windmill palm fibers had low cellulose contents (34.70–35.5%), low relative crystallinity index (45.7–49.2%), and high MFA (38.8°–29.4°), resulting in low strength and modulus, but high failure strain under tensile load. The tensile fracture surface of windmill palm fibers was assessed through SEM studies and its ductile fracture was confirmed, which can potentially enhance the toughness of composites when used as reinforcement material. Nanoindentation was carried out among different leaf sheath layers, and the results showed the modulus and hardness values of windmill palm fibers are in the same range as other plant fibers. The experimental results may help guide selection of suitable reinforcing fibers for use in composites in different applications.

**Keywords:** Windmill palm fiber, Fiber morphology, Mechanical properties, Nanoindentation

## Introduction

Over the last two decades, there has been a growing industrial interest in the development of lignocellulosic natural fibers as replacements for glass or other traditional reinforcement materials used in composites [1]. Natural fibers composites offer advantages of biodegradability, good accessibility, fast renewability, high specific properties, and low cost [2, 3]. However, a better understanding of the detailed morphology, structural, and mechanical properties of natural fibers is essential for evaluation of their potential as reinforcing materials in composites and optimization of the service life performance of composites [4].

*Correspondence: wanghankun@icbr.ac.cn
[2] Department of Biomaterials, International Center for Bamboo and Rattan, Beijing, People's Republic of China
Full list of author information is available at the end of the article

Windmill palm (*Trachycarpus fortunei*) is the most widely cultivated species at the latitudinal palm range margin, and distinguished by its large and fan-shaped leaves [5]. Every year, a portion of the leaves of the palm dries out to form a mesh of coarse and brown leaf sheath fiber that clasps the tree trunk, making it appear to be wrapped in burlap [6] (Fig. 1a). The palm leaf sheath fiber is considered an abundant agricultural byproduct due to the necessary regular pruning process of the palm tree by removing loose mats to keep the tree attractive and safe. Currently, due to their high durability and strength characteristics, palm fibers are used to make a variety of byproducts such as mattresses, sofas, marine ropes, sacks, and traditional raincoats [7]. However, these applications only utilize a small percentage of the total material produced, and the majority of the material is discarded directly as waste, causing serious environmental problems [8]. The possible use of palm fibers for composite


**Fig. 1** Photograph of **a** windmill palm tree covered with leaf sheath; **b** leaf sheath; **c** a small piece of leaf sheath showing the arrangements of different layers of fiber bundle, with inserted images showing the schematic view of fiber arrangement

reinforcement may provide a strategy for the efficient utilization of these waste fibers.

Each palm leaf sheath is composed of a middle layer of coarse fibers which is sandwiched between two layers of fibers with smaller diameters. There have been only preliminary studies of palm leaf sheath fibers. Zhang et al. [9] revealed a unique structure of palm fiber with sub-cylindrical shape containing abundant fiber cells in the cross section and Si-dots on the surface. Previously, the mechanical properties of palm fiber were mainly determined through monotonic tensile tests. Palm fiber exhibits excellent elongation properties, which is able to tolerate significantly higher stain than other natural fibers [10]. Chen et al. [11] investigated the influence of the chemical treatment of windmill palm fibers on its tensile properties, and found that alkalized fibers possessed higher tensile properties than untreated fibers. Nevertheless, none of these studies examined the potential variation in the physical and mechanical properties of palm fiber from different layers of the leaf sheath. Since there are three layers in each sheet of palm leaf sheath with some differences in terms of fiber morphology and tensile properties [12], it is important to assess the properties of these individual layers for a more comprehensive evaluation of the use of palm fiber as composite reinforcement material.

To facilitate reliable use of palm fiber in composites, a detailed investigation was performed of the mechanical properties of windmill palm fibers, separated from the three layers of leaf sheath, in relationship to their chemical composition and structural properties. First, the mechanical properties of palm fibers were determined at two scales: tensile tests at the fiber scale and nanoindentation tests at the cell wall scale. Next, microscopy (SEM) observation and X-ray diffraction were conducted to investigate morphology and structure (microfibrillar angle and relative degree of crystallinity), followed by chemical composition analysis. Finally, the results were considered in a detailed assessment of the relationships between the physical, chemical, and mechanical properties of the fiber.

## Materials and methods

### Sample preparation

Windmill palm tree trunk covered by leaf sheath was obtained from Anhui province, China (Fig. 1a). The leaf sheath fibers were mechanically separated from the petiole (Fig. 1b), and then washed with distilled water to remove impurities and dust and further air-dried to remove excessive water and moisture. Then, the cleaned leaf sheath was sorted into three layers, namely the outer, middle, and inner layers, according to their diameters and orientations (Fig. 1c). Comparison of sample preparation of different plant fibers is summarized in Additional file 1: Table S1.

### Morphological and chemical analysis

The longitudinal and transverse surface morphology of the palm fiber were investigated through SEM (XL30, FEI, USA) operating at 7 kV. The tensile fracture surface of the palm fibers was also analyzed. Before SEM observation, the samples were sputter-coated with a thin layer of Pt using an Edwards Sputter Coater.

The diameter and length of each palm fiber and elementary fiber were measured with a digital biological microscope (XTS20G, Fukai Ltd., China). In order to extract elementary fiber, palm fibers were chemically treated using a mixture solution of hydrogen peroxide and glacial acetic as described by Yu et al. [13]. For measurement of elementary fiber cell wall thickness, samples were embedded with Spurr resin and cut to obtain smooth transverse section for SEM observation.

The chemical composition (α-cellulose, hemicellulose, lignin, and ash content) of the palm fibers in different leaf sheath layers was analyzed in accordance with the Technical association of Pulp and Paper industry (TAPPI) standards, as described by Khalil et al. [14].

#### X-ray diffraction

A Philips X-ray diffraction system (X'pert Pro, PANalytical B.V., Almelo, NL) was used to evaluate both the microfibrillar angle (MFA) and relative crystallinity index (CrI) of palm fibers. Before measurement, palm fibers of the same layer were arranged closely to form a mat. Here, evaluation of the entire fiber was performed instead of examination of the powder samples that are commonly used in order to preserve the internal structure of the fibers [15]. Using Eq. (1), MFA of the palm fibers was determined by application of the widely used 0.6$T$ method [16]:

$$\mathrm{MFA} = 0.6 \times T, \tag{1}$$

where $T$-value was determined as half the width of the peak obtained in azimuthal distribution (Additional file 1: Fig. S1).

CrI was calculated as described by Segal et al. [17], as follows:

$$\mathrm{CrI} = (I_{002} - I_{\mathrm{am}})/I_{002}, \tag{2}$$

where $I_{002}$ is the maximum intensity of the 002 peak at $2\theta$ about 22° and $I_{\mathrm{am}}$ is the minimum intensity of diffraction of the amorphous materials at $2\theta$ about 18°.

#### Tensile tests

Tensile tests were first conducted in a universal mechanical testing machine (Instron Microtester 5848, USA) using a 500 N load cell. Before the tensile test, two palm fiber ends were glued with instant epoxy adhesive onto a piece of poplar veneer to avoid any specimen sliding from the clamps. A gauge length of 50 mm was selected and elongation was recorded with a non-contacting video extensometer by tracking two small black speckles marked on the sample. For each layer of fibers, at least 30 fibers were tested. Tensile tests were conducted under an environment of 20 °C and 30% relative humidity (RH). To calculate the tensile strength and modulus of palm fibers, the cross-sectional area of the samples was assessed with a digital microscope (XTS20G, Fukai LTD., China) and then measured with an image-processing software (Image-ProPlus 5.0, Media Cybernetics, USA).

#### Nanoindentation testing

For nanoindentation testing, palm fibers were embedded in Spurr resin and cured in a flat mold as previous described [13]. After curing, the embedded samples were polished with a glass knife and a diamond knife to prepare a smooth surface exposing a transverse section. The nanoindentation experiments were performed using a Triboindenter (Hysitron Incorporation, USA) with a diamond Berkovich indenter (tip radius less than 100 nm). The indentation procedure was performed under load control using a three-segment load ramp: reaching the peak load of 150 μN within 6 s, holding at the peak load for 6 s, and then unloading within 3 s. In total, 20–25 indentations were conducted for each layer of palm fibers. The elastic modulus and hardness were calculated from the experimental curves according to the method developed by Oliver and Pharr [18].

## Results and discussion

### Fiber morphology

A windmill palm trunk is covered with a large amount of leaf sheath (Fig. 1a), and each leaf sheath can be easily separated into three layers of fibers due to the orderly arrangements (Fig. 1c). The fiber size differs in different layers of palm fibers (listed in Table 1): the middle layer contained the largest size of fibers (516 ± 40 μm), followed by the outer layer (372 ± 75 μm), and the inner layer (230 ± 37 μm). Also, morphological differences were detected by cross-sectional SEM observation, as the fibers from the inner layer showed a homogeneous structure almost completely comprising numerous single elementary fiber (Fig. 2a), whereas the fibers from the middle and outer layers exhibited clear vessels and phloem tissue (conducting tissues) surrounded by elementary fibers (Fig. 2b, c). This specific organization of fibers in different layers is likely related to their different functions, as the small fibers in the inner layer, which closely clasps the palm trunk, mainly play a structural

**Table 1 Fiber and elementary fiber sizes in different palm leaf sheath layers**

| Leaf sheath layer | Fiber | Elementary fiber | | |
|---|---|---|---|---|
| | Diameter (μm) | Diameter (μm) | Length (μm) | Cell wall thickness (μm) |
| Inner layer | 230 ± 37 | 12.1 ± 1.9 | 932 ± 164 | 2.2 ± 0.3 |
| Middle layer | 516 ± 40 | 13.1 ± 1.9 | 1019 ± 160 | 1.7 ± 0.3 |
| Outer layer | 372 ± 75 | 12.7 ± 1.5 | 989 ± 178 | 2.2 ± 0.3 |

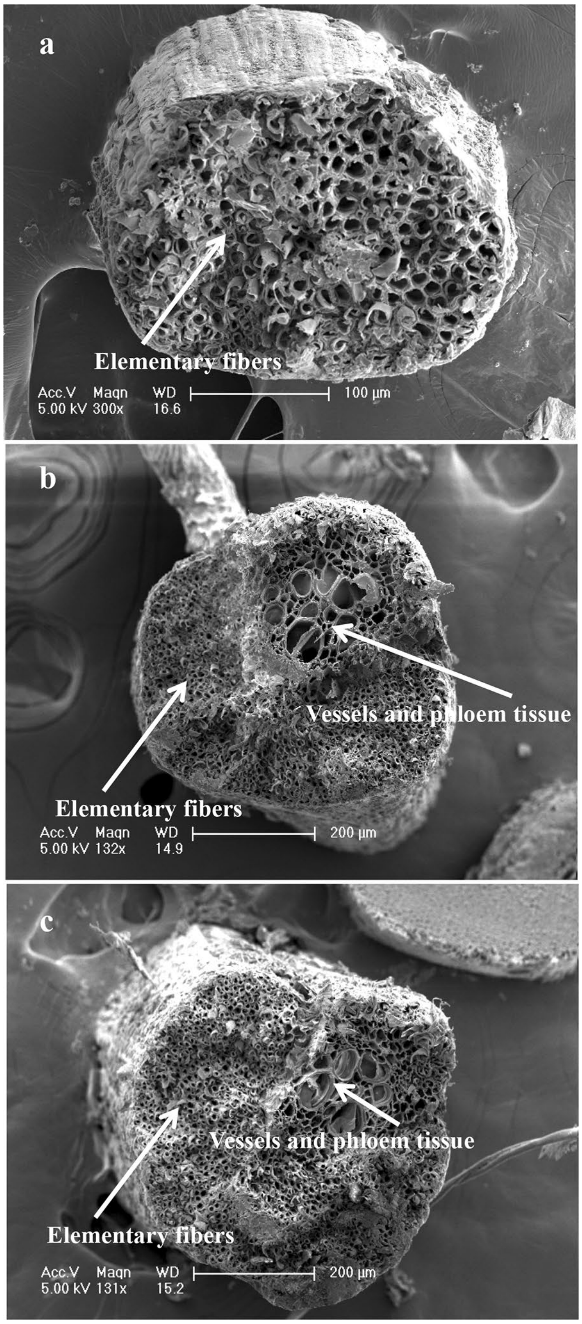


**Fig. 2** SEM images of palm fibers in different layers: **a** inner layer, **b** middle layers, **c** outer layer

role, and the large fibers in the outer and middle layers facilitate the transportation of nutrients through the conductive tissues. Unlike the observed variability of fiber diameters and morphology, the dimensions of elementary fiber were similar among the different layers, with average diameters ranging from 12.1 to 13.1 µm, and fiber length ranging from 930 to 1019 µm, and cell wall thickness ranging from 1.7 to 2.2 µm. A similar observation was reported by Zhai et al. [12] previously.

There was similar surface morphology of palm fibers in different layers. For example, in a fiber sample from the outer layer, the fiber was sub-cylindrical in shape (Fig. 3a) with a large number of wax and impurities on the rough surface (Fig. 3b). In some cleaner areas, the surface was covered by arrays of protrusions (Fig. 3c), identified as silica bodies embedding circular craters under higher magnification (Fig. 3d) which had been confirmed through energy dispersive X-rays spectrometry (EDS) [19]. Similar features were also observed in other palm trees, such as piassava palm fibers [20], date palm fibers [21], and sugar palm fibers [22]. The main function of these silica bodies is to protect the external surface of the fiber from pathogenic fungi and insects, but the presence of the silica may interfere with pulping and papermaking [21]. However, the silica bodies do not stick firmly onto the fiber and can be removed mechanically, leaving empty craters that may facilitate mechanical interlocking of the fiber and matrix due to the rougher surface [2].

### Chemical composition and structural properties

The chemical composition of windmill palm fibers in various leaf sheath layers is detailed in Table 2, and the composition of other palm family fibers and some commonly used fibers are presented for comparison. Like other natural fibers, analysis showed that the palm fibers were composed mainly of cellulose, hemicellulose, and lignin, with similar contents among the different layers of leaf sheath. The remarkable consistency of the composition was in contrast to the dramatic variations reported in fiber diameter and cross-sectional morphology. Windmill palm has a relatively lower cellulose content (34.3–35.5%) compared to other members of the palm family, such as oil palm (42.7–65.0%) [2], and sugar palm (43.8–44.5%) [23], but a level comparable with piassava palm (31.6%) [20]. Compared with flax, jute, and sisal fibers [24], windmill palm fiber has a relative higher lignin content that is comparable to that of other palm family fibers, except oil palm. The high lignin content may contribute to its brown color and useful properties such as weather, fungal, and bacterial resistance [19].

The MFA, the spiral angle between the cellulose fibrils and the fiber axial, is considered an influential structural parameter that affects the axial mechanical properties of natural fibers [25]. The measured MFA values of palm fibers were in the range of $38.8 \pm 1.5°$ for the inner layer to $39.4 \pm 1.0°$ for the outer layer, which were very similar and reproducible values (Table 2). The CrI of windmill palm fibers was found to vary slightly for the different layers, with the highest in the middle layers (49.2%), followed by the outer layers (46.7%), and finally the inner

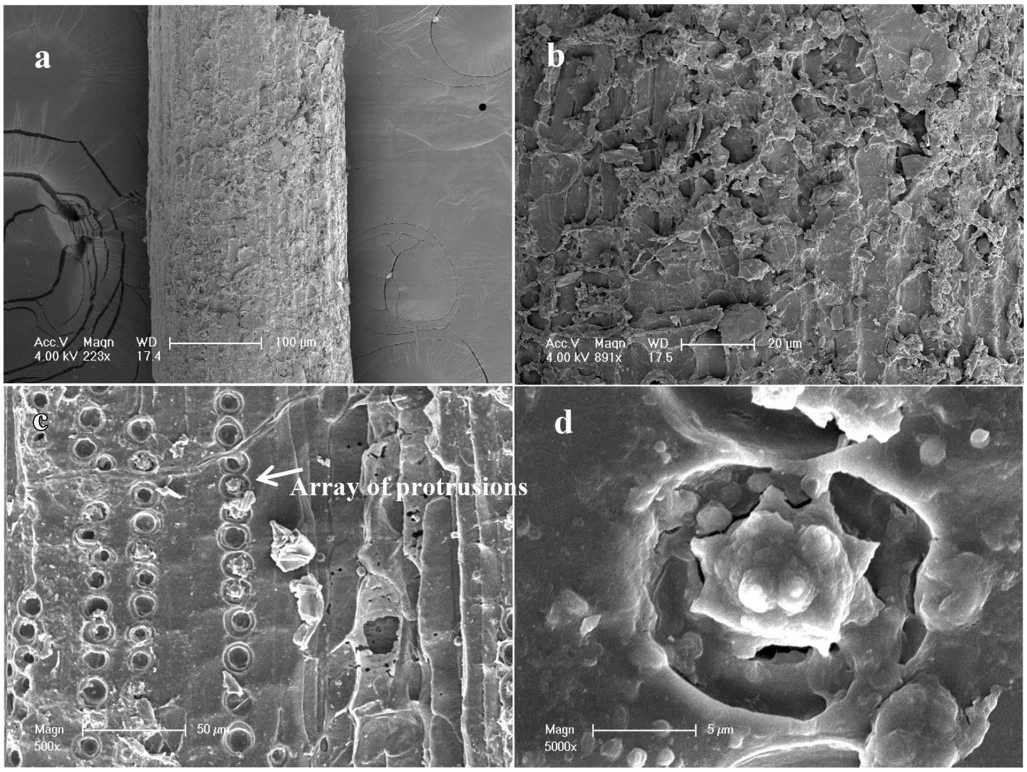


**Fig. 3** Surface morphological characterizations of palm fibers in outer layer: **a** sub-cylindrical shape, **b** waxy and course surface, **c** arrays of protrusions embedded with **d** silica

**Table 2 Comparison of properties of windmill palm fibers with other natural fibers**

| Natural fibers | Chemical composition (%) | | | | Structural characterization | | Tensile properties | | |
|---|---|---|---|---|---|---|---|---|---|
| | α-Cellulose | Hemicellulose | Lignin | Ash | MFA(°) | CrI (%) | Tensile modulus (GPa) | Tensile strength (MPa) | Failure strain (%) |
| Windmill palm (this study) | | | | | | | | | |
| Inner layer | 35.5 | 22.5 | 36.4 | 1.4 | 38.8 ± 1.5 | 45.7 | 3.5 ± 0.8 | 132.0 ± 27.8 | 17.6 ± 2.9 |
| Middle layer | 34.3 | 24.7 | 36.8 | 3.9 | 39.2 ± 1.3 | 49.2 | 2.7 ± 0.4 | 73.7 ± 17.2 | 10.5 ± 2.9 |
| Outer layer | 34.7 | 25.3 | 38.3 | 1.1 | 39.4 ± 1.0 | 46.7 | 2.9 ± 0.5 | 72.8 ± 21.2 | 10.0 ± 4.7 |
| Windmill palm [9, 12] | 28.2 | 20.6 | 44.1 | – | 37.8–42.2 | 30.5–73 | 0.3–1.3 | 82.1–170.1 | 22.6–55.2 |
| Date palm [21] | 45 ± 3 | 28 ± 2 | 17 ± 0.3 | 1.7 ± 0.1 | 26.1 ± 14.2 | 41 ± 3 | 1.8 ± 0.6 | 131 ± 34 | 20.9 ± 7.6 |
| Oil palm [2] | 42.7–65 | 17.1–33.5 | 13.2–25.31 | 1.3–6.0 | 46 | – | 0.6–9 | 50–400 | 4–18 |
| Sugar palm [23] | 43.8–44.5 | 8.9–10.0 | 39.5–41.9 | 0.9–1.3 | – | – | 3.9–4.3 | 211–233 | 15.8–20.6 |
| Piassava palm [20] | 31.6 | – | 48.4 | – | – | – | 2.6 ± 0.4 | 131.1 ± 27.1 | 11.9 ± 4.3 |
| Coir [35] | 34.3–53.6 | 29.1–22.3 | 24–36.4 | – | – | 37.1–39 | 4.8–18 | 94.3–119.8 | 5.5–6.3 |
| Flax [24] | 72.6 | 8.7 | 3.2 | – | 4.5 | – | 20.8 | 520 | 1.9 |
| Jute [24] | 46.2 | 12.5 | 15.4 | – | 8 | – | 24.6 | 390 | 1.5 |
| Sisal [24] | 45.3 | 20.4 | 15.1 | – | 20 | – | 18.7 | 400 | 2.7 |

layer (45.7%). These results are similar to those reported by Zhai et al. [12], Zhang et al. [9].

### Tensile properties

The typical stress–strain curves of palm fibers obtained from each leaf sheath layer are presented in Fig. 4, and their tensile properties are listed in Table 2. The curves show that the palm fibers all exhibited linear elastic at low stress, and then yielding point at around 2% strain followed by plastic deformation until breakage, and similar results have been reported for piassava fiber [19] and coir fiber [4]. There were some evident differences in the mechanical properties of palm fibers among the different leaf sheath layers, as shown in Table 2. Some large variations in the tensile properties of palm fibers can be found in all three layers, which are often observed for natural fibers published by other authors [7, 21]. In general, the average tensile modulus, stress, and failure strain of the fibers in the inner layer were much higher than those in fibers from the outer and middle layers. As the crystalline cellulose confers the stiffness and strength (around 135 GPa) [26], the superior tensile properties of natural fibers have been attributed to the high cellulose content and crystallinity, and the comparatively low MFA [27]. However, the cellulose content, CrI and MFA values were in similar ranges among different layers of windmill palm fibers (Table 2). Therefore, the differences in mechanical properties between layers may be more associated with the morphological parameters, as obvious variations in fiber morphology, particularly fiber diameter, were observed between different leaf sheath layers (Table 1). Fibers in the inner layers had the smallest diameter and exhibited superior mechanical properties among the three layers. Consistently, earlier studies showed significant correlations between mechanical properties and fiber diameter, and a decreased trend in mechanical properties was observed for increasing fiber diameters [12, 28]. As assayed here, windmill palm fibers exhibited higher tensile modulus, but lower failure strain compared with previously reported results [9, 12].

As shown in Table 2, windmill palm fibers exhibited significantly lower tensile modulus and strength compared with those of flax, jute, and sisal [24], but values that were much closer to that of other palm family fibers, such as date palm [21] and especially piassava fiber [20]. This is expected as windmill palm fibers have lower cellulose content (34.3–35.5%), lower CrI (45.7–49.2%), and higher MFA values (38.8°–39.4°). However, unlike

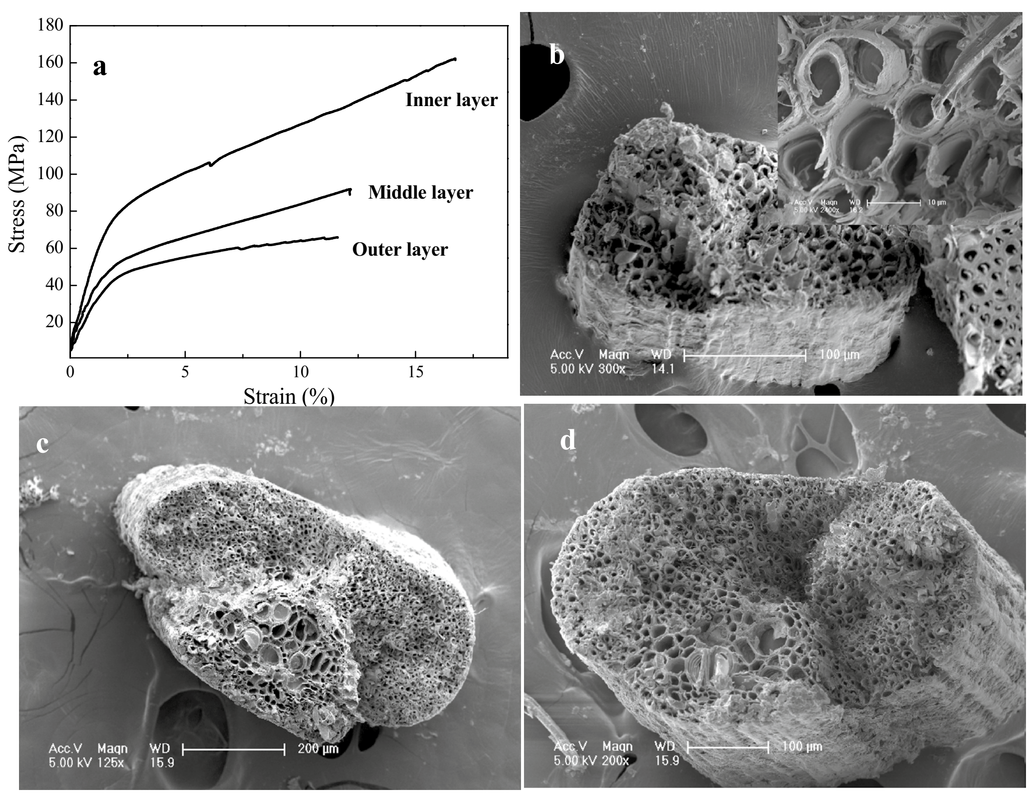


**Fig. 4** **a** Typical stress–strain curves of windmill palm fibers in different layers; fracture surface of fiber in **b** inner, **c** middle, and **d** outer layer of one windmill palm leaf sheath

these stiffer and stronger fibers that exhibit brittle failure at relatively low ultimate tensile strain (Table 2), windmill palm fibers showed ductile failure with a large failure strain of 10.0–17.6% with dissipated strain energy. The ductile behavior of windmill palm fiber was related to its fracture mode, as shown in Fig. 4b–d. The failure of the fibers is caused by the fracture of the cell wall with delamination, as shown in the inset in Fig. 4b. Similar intercellular fracture has also been reported for other fibers with a low cellulose content and high MFA, such as coir and piassava fiber [29].

The use of windmill palm fibers as reinforcement material in composites is perhaps not an obvious choice due to its relatively lower tensile modulus and strength compared to other widely used fibers. However, although the addition of windmill palm fiber may not enhance the stiffness and strength of a composite, it can improve the toughness of the material due to its high failure strain. Additionally, waste windmill palm fiber can be incorporated with a strong–brittle fiber (such as jute or flax) into a polymer matrix to produce a hybrid composite, in which the palm fibers exhibit high failure strain which allows better stress transfer, and provides large diameter material to increase the effective fiber–matrix adhesion area [30]. As mentioned above, the windmill palm fibers share strong similarities with coir and piassava fiber, and these two fibers have been successfully used as reinforcement materials [31, 32], which strongly suggests that the windmill palm may be an excellent reinforcement material to improve the properties of composites.

#### Nanoindentation testing

Nanoindentation is a powerful tool to characterize mechanical properties on a very small scale [33]. The typical load–depth curves of the windmill palm fibers in different leaf sheath layer were determined and shown in Fig. 5a. Fibers in the inner layers reached a much lower maximum depth (ca. 96 nm) compared to those from the middle and outer layers (ca. 145 nm), however, the final depth of these fibers were similar (ca. 70 nm) after the

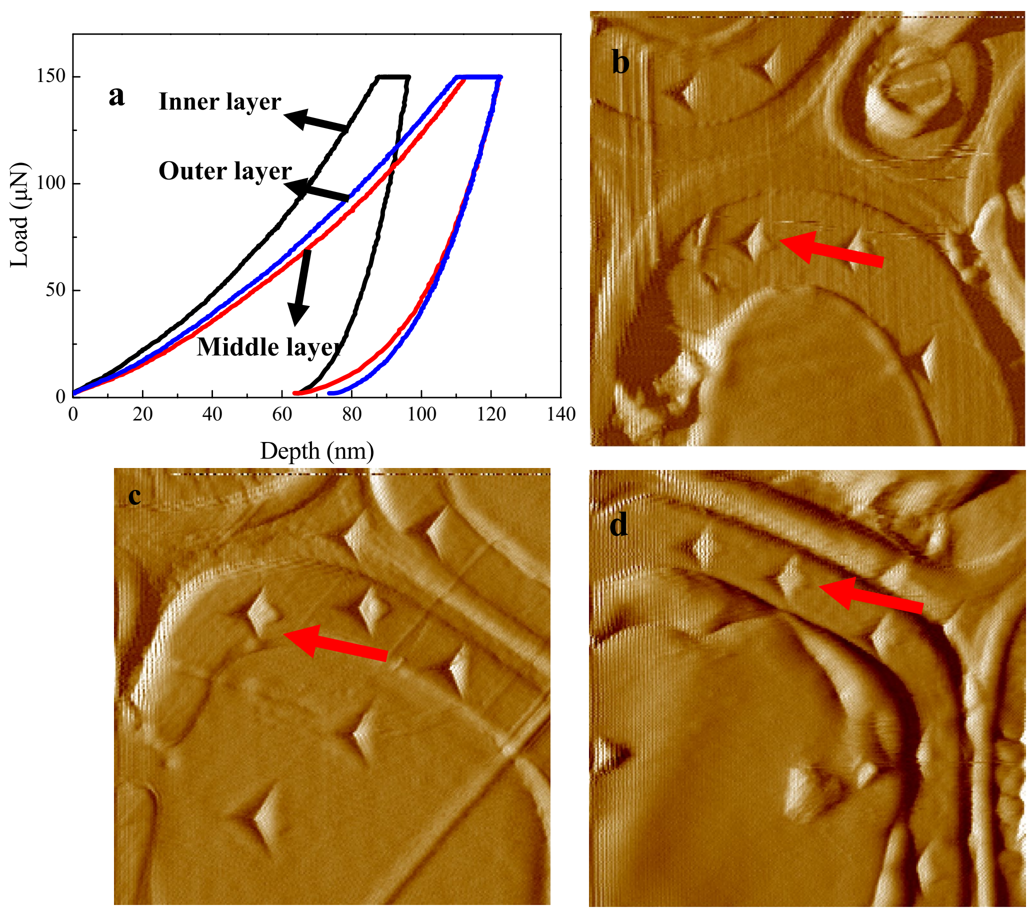


**Fig. 5** **a** Typical load–depth curves of nanoindentation tests in cell wall of windmill palm fibers in different layers; Residual indentations on cell wall of windmill palm fibers in **a** inner, **b** middle, **c** outer layer

unloading process, which indicated different viscoelastic behavior among different layers. Figure 5b–d exhibits the indented areas of the fiber cell wall in three layers, and only indents located in the cell (marked by red arrows) were considered acceptable.

The longitudinal elastic modulus and hardness of palm cell walls in three layers are shown in Table 3. Palm fibers in inner layers showed much higher value in elastic modulus (13.2 GPa) and hardness (0.5 GPa) than that of palm fibers in the middle and outer layers. In general, the mechanical properties of the fiber cell wall are positively related to lignin content and negatively correlated with MFA values [34]. However, despite palm fiber in inner and outer layer exhibited no appreciable differences in chemical composition, MFA, CrI values (Table 2), as well as elementary fiber size and cell wall thickness values (Table 1), their nanoindentation properties exhibited significant differences. The diameter of fiber in inner layer was much smaller (230 μm) than that of fiber in outer layer (372 μm), which indicated that fiber diameter could be important contributors to the difference. Similar results have been observed for the two types of leaf sheath fiber identified in date palm, where small fiber bundles (70–120 μm) exhibited superior nanoindentation properties than large fiber bundles (600–1200 μm), which might be related to their mechanical role in leaf sheath [21]. The nanoindentation properties of windmill palm fiber were in the same range with those of crops and wood, and comparable to those of date palm [21], as shown in Table 2. This may be partly explained by the remarkable high lignin content in the windmill palm fibers, which makes the fiber cell wall rigid.

**Table 3 Comparison of nanoindentation properties of windmill palm fiber with other natural fibers**

| Natural fibers | Nanoindentation modulus (GPa) | Nanoindentation hardness (GPa) |
|---|---|---|
| Windmill palm (this study) | | |
| Inner layer | 13.2 ± 1.3 | 0.50 ± 0.04 |
| Middle layer | 8.9 ± 0.8 | 0.37 ± 0.04 |
| Outer layer | 8.5 ± 0.9 | 0.36 ± 0.03 |
| Windmill palm [11] | 7.6 ± 4.0 | 0.13 ± 0.02 |
| Date palm [21] | 14.3–15.8 | 0.47–0.53 |
| Crops (cotton stalk, cassava stalk, soybean stalk, rice straw, hemp stalk) [36] | 12.3–20.8 | 0.41–0.85 |
| Hardwood (poplar, iroko, alder birch, Manchurian ash, Asian white birch, red oak, white oak, Mongolian oak, kwila, keranji) [37] | 16.9–24.6 | 0.44–0.56 |
| Softwood (loblolly pine, spruce) [36] | 14.2–18 | 0.34–0.53 |

## Conclusions

The fiber morphology, chemical composition, physical, and multi-scale mechanical properties of windmill palm fibers in three leaf sheath layers were investigated in this study. The tensile and nanoindentation properties of fine fibers in the inner leaf sheath layer were highest among the three layers, which may reflect their mechanical role in leaf sheath. The palm fibers are not as strong and stiff, but exhibit a high elongation at break. The nanoindentation results revealed that the modulus and hardness of windmill palm fiber were comparable to those of wood and crops fibers. These results will help promote the use of windmill palm fiber as a material from renewable resources with more high-value applications.

## Supplementary information

**Supplementary information** accompanies this paper at https://doi.org/10.1186/s10086-020-1851-z.

**Additional file 1: Table S1.** Comparison of sample preparation of different plant fibers. **Figure S1.** Azimuthal distribution of palm fiber at different layers.

### Abbreviations

SEM: scanning electron microscopy; MFA: microfibrillar angle; CrI: relative crystallinity index.

### Acknowledgements

Not applicable.

### Authors' contributions

JL performed the experiments and wrote the majority of the manuscript. XZ interpreted the results and wrote a part of the manuscript. JZ collected the samples and discussed the results. YY designed the experiments and interpreted the results. HW supervised the overall work. All authors read and approved the final manuscript.

### Funding

This work was supported by Basic Scientific Research Funds of International Center for Bamboo and Rattan (1632018017) and the 12th five years key technology R&D program (2015BAD04B03).

### Availability of data and materials

The datasets used and/or analyzed during the current study are available from the corresponding author on reasonable request.

### Ethics approval and consent to participate

Not applicable.

### Consent for publication

Not applicable.

### Competing interests

The authors declare that they have no competing interests.

### Author details

[1] Key Lab of Wood Science and Technology of National Forestry and Grassland Administration, Research Institute of Wood Industry, Chinese Academy of Forestry, Beijing, People's Republic of China. [2] Department of Biomaterials, International Center for Bamboo and Rattan, Beijing, People's Republic of China. [3] SFA and Beijing Co-built Key Lab for Bamboo and Rattan Science & Technology, Beijing, People's Republic of China. [4] College of Material

Engineering, Fujian Agriculture and Forestry University, Fuzhou 350002, People's Republic of China.

Received: 29 September 2019 Accepted: 16 January 2020
Published online: 04 February 2020

**References**


1. Gurunathan T, Mohanty S, Nayak SK (2015) A review of the recent developments in biocomposites based on natural fibres and their application perspectives. Compos Part A Appl Sci. 77:1–25
2. Shinoj S, Visvanathan R, Panigrahi S, Kochubabu M (2011) Oil palm fiber (opf) and its composites: a review. Ind Crop Prod 33(1):7–22
3. Berges M, Léger R, Placet V, Person V, Corn S, Gabrion X, Rousseau J, Ramasso E, Lenny P, Fontaine S (2016) Influence of moisture uptake on the static, cyclic and dynamic behaviour of unidirectional flax fibre-reinforced epoxy laminates. Compos Part A Appl Sci 88:165–177
4. Tran LQN, Minh TN, Fuentes CA, Chi TT, Vuure AWV, Verpoest I (2015) Investigation of microstructure and tensile properties of porous natural coir fibre for use in composite materials. Ind Crop Prod 65:437–445
5. Walther G, Gritti ES, Berger S, Hickler T, Tang Z, Sykes MT (2010) Palms tracking climate change. Global Ecol Biogeogr. 16(6):801–809
6. Gilman E, Watson D (2015) *Trachycarpus fortunei*: windmill palm. Environmental Horticulture. ENH-802. UF/IFAS Extension Service, University of Florida
7. Zhai S, Sugiyama J, Imai T, Horikawa Y (2013) Cell wall characterization of windmill palm (*Trachycarpus fortunei*) fibers and its functional implications. IAWA J 34(1):20–33
8. Chen CJ, Zhang Y, Jia J, Wang M, Wang G (2015) Morphology research of windmill palm (*Trachycarpus fortunei*) material. Kem Ind 64(9–10):467–472
9. Zhang T, Guo M, Cheng L, Li X (2015) Investigations on the structure and properties of palm leaf sheath fiber. Cellulose 22(2):1039–1051
10. Guo M, Zhang TH, Chen BW, Cheng L (2014) Tensile strength analysis of palm leaf sheath fiber with Weibull distribution. Compos Part A Appl Sci 62(17):45–51
11. Chen C, Chen G, Li X, Guo H, Wang G (2017) The influence of chemical treatment on the mechanical properties of windmill palm fiber. Cellulose 24(4):1611–1620
12. Zhai S, Li D, Pan B, Sugiyama J, Itoh T (2012) Tensile strength of windmill palm (*Trachycarpus fortunei*) fiber bundles and its structural implications. J Mater Sci 47(2):949–959
13. Yu Y, Tian G, Wang H, Fei B, Wang G (2011) Mechanical characterization of single bamboo fibers with nanoindentation and microtensile technique. Holzforschung 65(65):113–119
14. Khalil HPSA, Yusra AFI, Bhat AH, Jawaid M (2010) Cell wall ultrastructure, anatomy, lignin distribution, and chemical composition of malaysian cultivated kenaf fiber. Ind Crop Prod 31(1):113–121
15. Marrot L, Lefeuvre A, Pontoire B, Bourmaud A, Baley C (2013) Analysis of the hemp fiber mechanical properties and their scattering (Fedora 17). Ind Crop Prod 51(6):317–327
16. Stuart SA, Evans R (1995) X-ray diffraction estimation of the microfibril angle variation in eucalypt wood. Appita J 48(3):197–200
17. Segal L, Creely J, Martin A, Conrad C (1959) An empirical method for estimating the degree of crystallinity of native cellulose using the X-ray diffractometer. Text Res J 29(10):786–794
18. Oliver WC, Pharr GM (1992) An improved technique for determining hardness and elastic modulus using load and displacement sensing indentation experiments. J Mater Res 7:1564–1583
19. D'Almeida JRM, Aquino RCMP, Monteiro SN (2006) Tensile mechanical properties, morphological aspects and chemical characterization of piassava (*Attalea funifera*) fibers. Compos Part A App Sci 37(9):1473–1479
20. Nascimento DCO, Ferreira AS, Monteiro SN, Aquino RCMP, Kestur SG (2012) Studies on the characterization of piassava fibers and their epoxy composites. Compos Part A Appl Sci 43(3):353–362
21. Bourmaud A, Dhakal H, Habrant A, Padovani J, Siniscalco D, Ramage MH, Beaugrand J, Shah DH (2017) Exploring the potential of waste leaf sheath date palm fibres for composite reinforcement through a structural and mechanical analysis. Compos Part A Appl Sci 103:292–303
22. Rashid B, Leman Z, Jawaid M, Ghazali MJ, Ishak MR (2016) Physicochemical and thermal properties of lignocellulosic fiber from sugar palm fibers: effect of treatment. Cellulose 23(5):2905–2916
23. Huzaifah MRM, Sapuan SM, Leman Z, Ishak MR (2017) Comparative study on chemical composition, physical, tensile, and thermal properties of sugar palm fiber (*Arenga pinnata*) obtained from different geographical locations. BioResources 12(4):9366–9382
24. Guen MJL, Newman RH, Fernyhough A, Hill SJ, Staiger MP (2016) Correlations between the physiochemical characteristics of plant fibres and their mechanical properties. In: Fangueiro R, Rana S (eds) Natural fibres: advances in science and technology towards industrial applications. RILEM Bookseries, vol 12. Springer, Dordrecht
25. Yu Y, Wang H, Fang L, Tian G, Lin J (2014) Bamboo fibers for composite applications: a mechanical and morphological investigation. J Mater Sci 49(6):2559–2566
26. Kroon-Batenburg LMJ, Kroon J, Northolt MG (1986) Chain modulus and intramolecular hydrogen bonding in native and regenerated cellulose fibres. Polym Commun 27(10):290–292
27. Djafari SR (2017) Physical and mechanical properties of natural fibers. In: Fan M (ed) Advanced high strength fibre composites in construction, 1st edn. Elsevier, Cambridge
28. Placet V, Trivaudey F, Cisse O, Gucheret-Retel V, Boubakar ML (2012) Diameter dependence of the apparent tensile modulus of hemp fibres: a morphological, structural or ultrastructural effect? Compos Part A Appl Sci 43:275–287
29. Satyanarayana KG, Flores-Sahagun THS, Bowman P (2018) Lignocellulosic materials of Brazil-their characterization and applications in polymer composites and art works. In: Kalia S (ed) Lignocellulosic composite materials. Springer series on polymer and composite materials. Springer, Cham
30. Gupta MK, Srivastava RK (2016) Mechanical properties of hybrid fibers-reinforced polymer composite: a review. Polym Plast Technol 55(6):17
31. Reis JML, Motta EP (2014) Mechanical behavior of piassava fiber reinforced castor oil polymer mortars. Compos Struct 111(1):468–472
32. Yan L, Chouw N, Huang L, Kasal B (2016) Effect of alkali treatment on microstructure and mechanical properties of coir fibres, coir fibre reinforced-polymer composites and reinforced-cementitious composites. Constr Build Mater 112:168–182
33. Jäger A, Bader T, Hofstetter K, Eberhardsteiner J (2011) The relation between indentation modulus, microfibril angle, and elastic properties of wood cell walls. Compos Part A Appl Sci 42(6):677–685
34. Li X, Wang S, Du G, Wu Z, Meng Y (2013) Variation in physical and mechanical properties of hemp stalk fibers along height of stem. Ind Crop Prod 42:344–348
35. Reddy KO, Reddy GS, Maheswari CU, Rajulu AV, Rao KM (2010) Structural characterization of coconut tree leaf sheath fiber reinforcement. J Forestry Res 21(1):53–58
36. Wu Y, Wang S, Zhou D, Xing C, Zhang Y, Cai Z (2010) Evaluation of elastic modulus and hardness of crop stalks cell walls by nano-indentation. Bioresour Technol 101(8):2867–2871
37. Wu Y, Wang S, Zhou D, Xing C, Zhang Y (2009) Use of nanoindentation and silviscan to determine the mechanical properties of 10 hardwood species. Wood Fiber Sci 41(1):64–73


## Publisher's Note